RSC Advances

ROYAL SOCIETY OF CHEMISTRY

www.rsc.org/advances

Table 1 Textural properties of DP and IMP catalysts.

DP Catalyst	DP-0	DP-1	DP-2	DP-3	DP-4	DP-5
S_{BET} (m^2 g^{-1})[a]	809.10	635.90	619.05	614.09	612.77	597.16
Pd dispersion (%)[b]	39.40	72.79	84.23	76.07	55.31	44.02
IMP Catalyst	IMP-0	IMP-1	IMP-2	IMP-3	IMP-4	IMP-5
S_{BET} (m^2 g^{-1})[a]	842.31	634.54	624.03	610.29	603.99	598.00
Pd dispersion (%)[b]	20.41	23.84	23.17	23.43	22.34	22.44

a. Surface area determined by N_2 adsorption using the Brunauer-Emmett-Teller (BET) method.

b. Measured by CO chemisorption.

Fig. 1

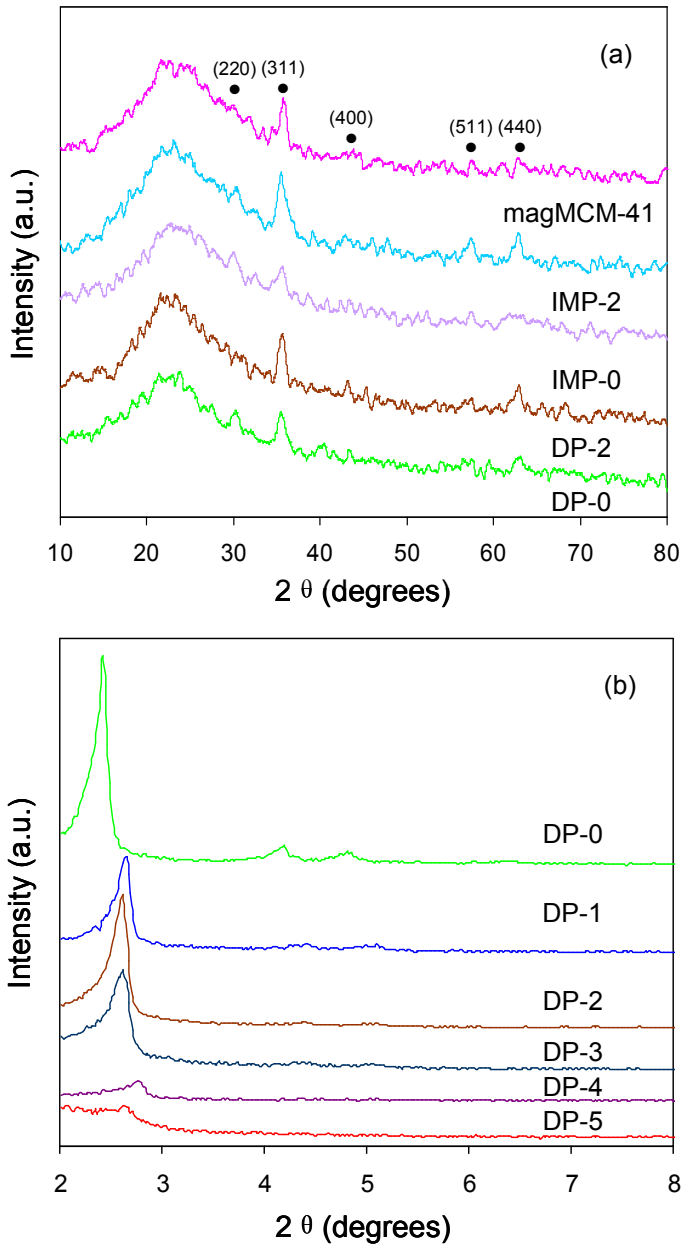

Fig. 2

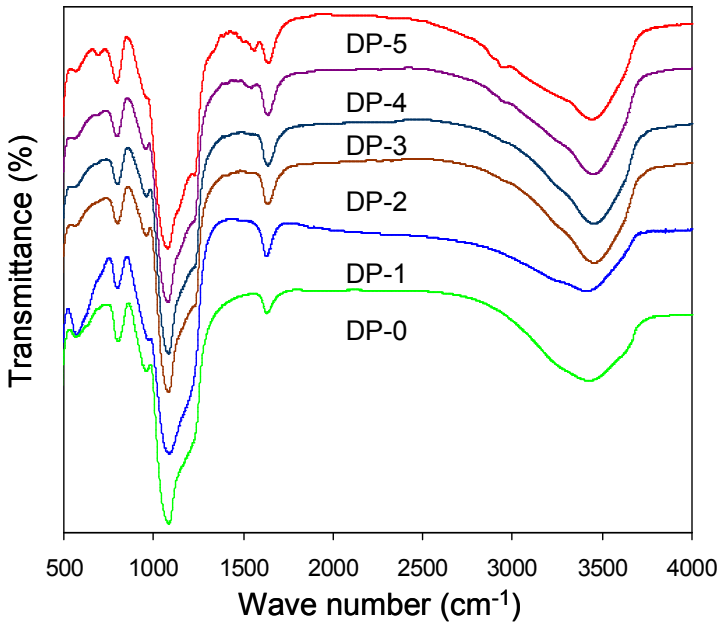

Fig. 3

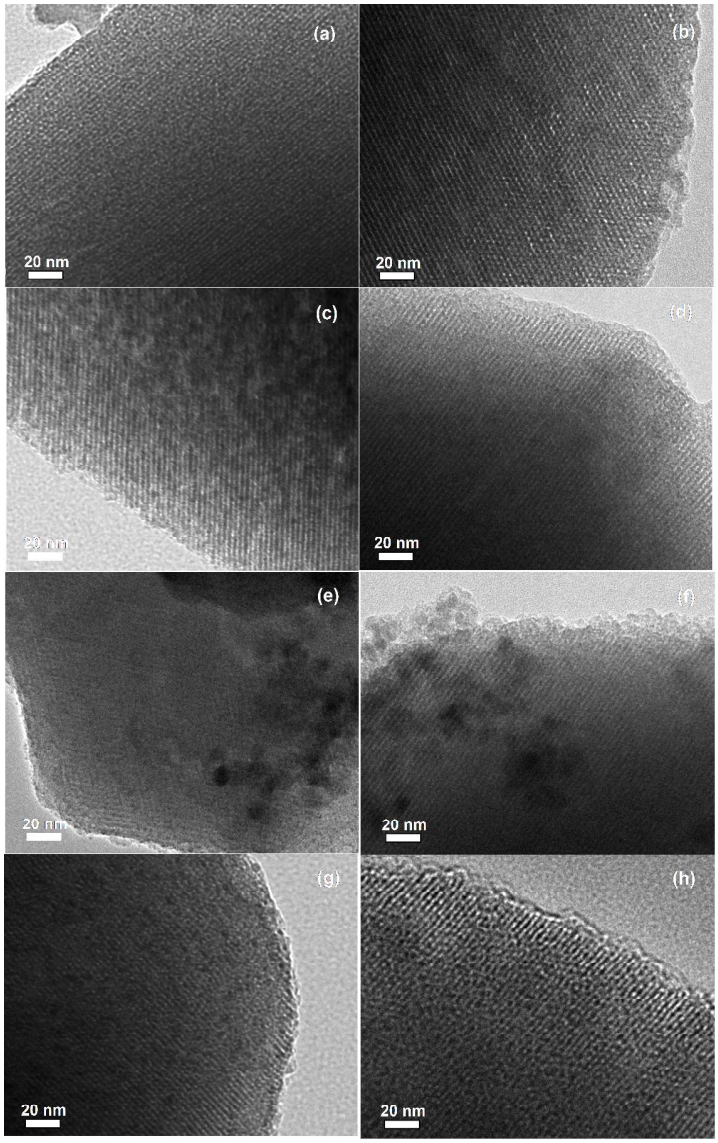

Fig. 4

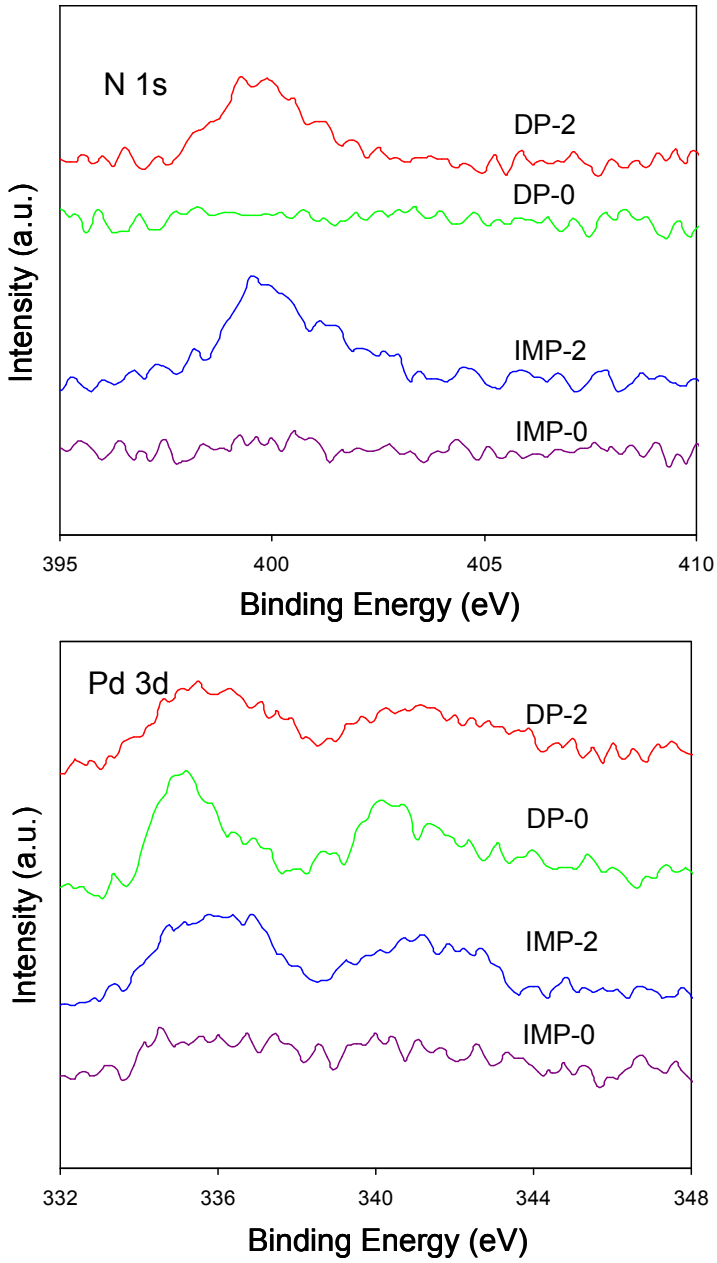

Fig. 5

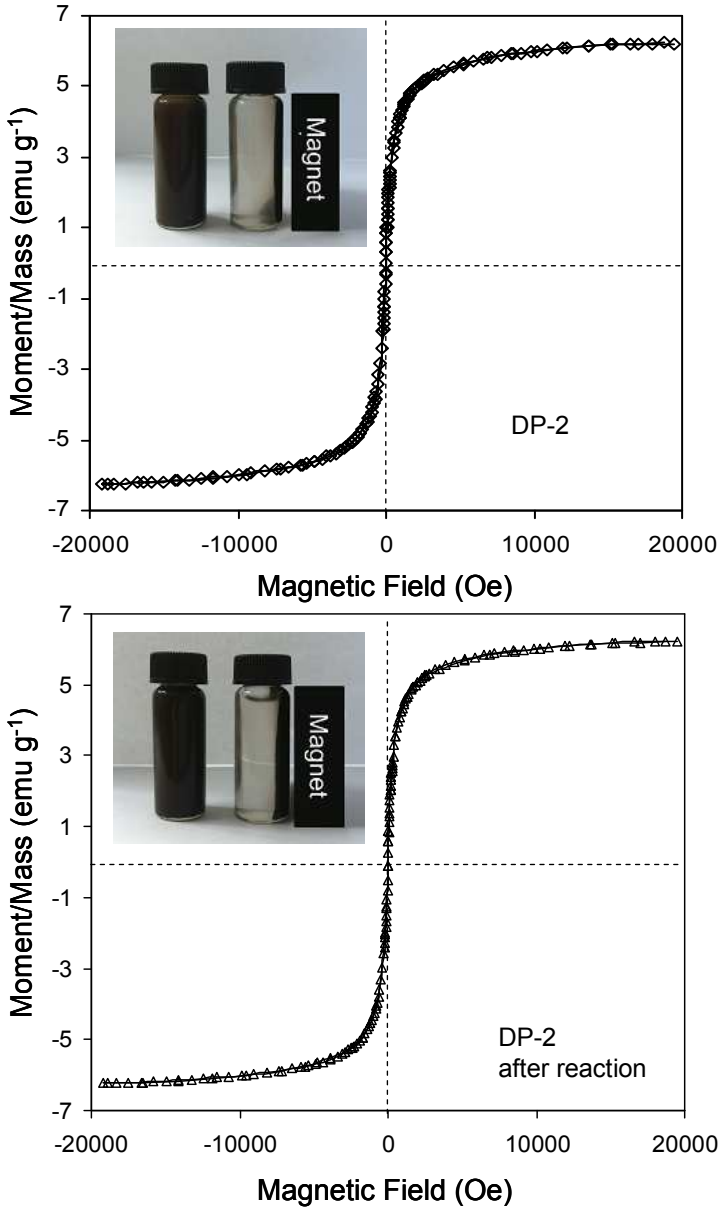

Fig. 6

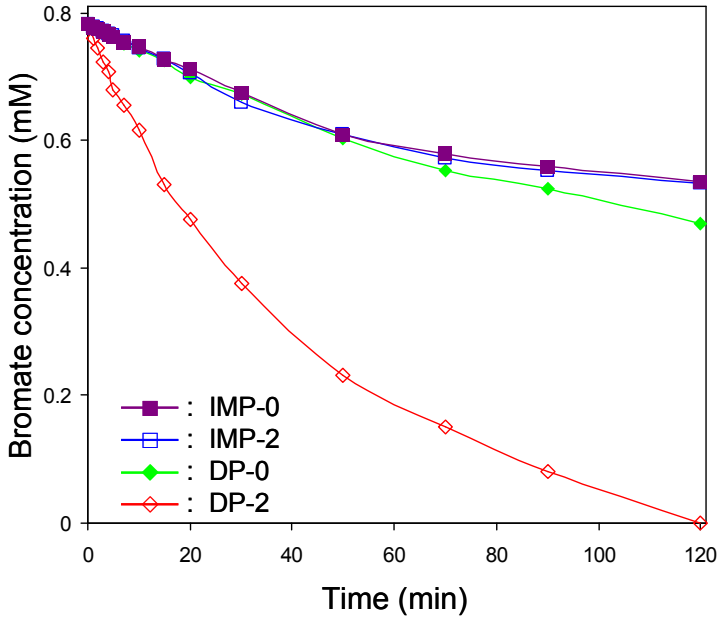

Fig. 7

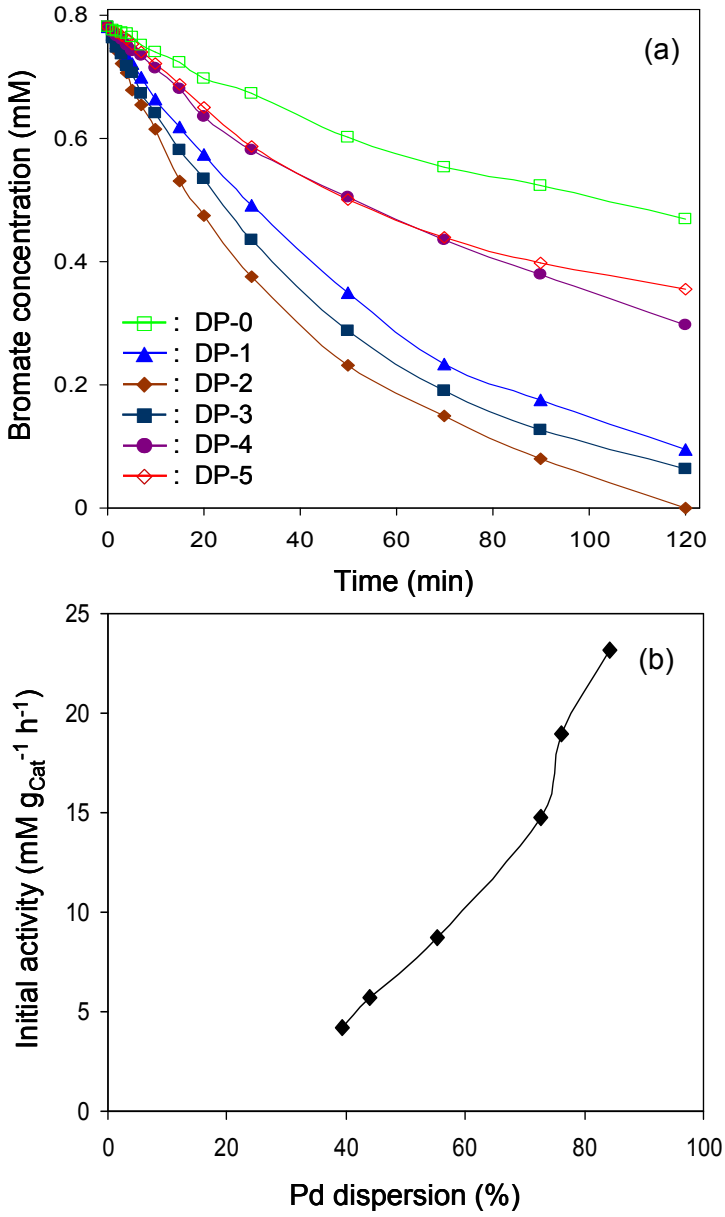

Fig. 8

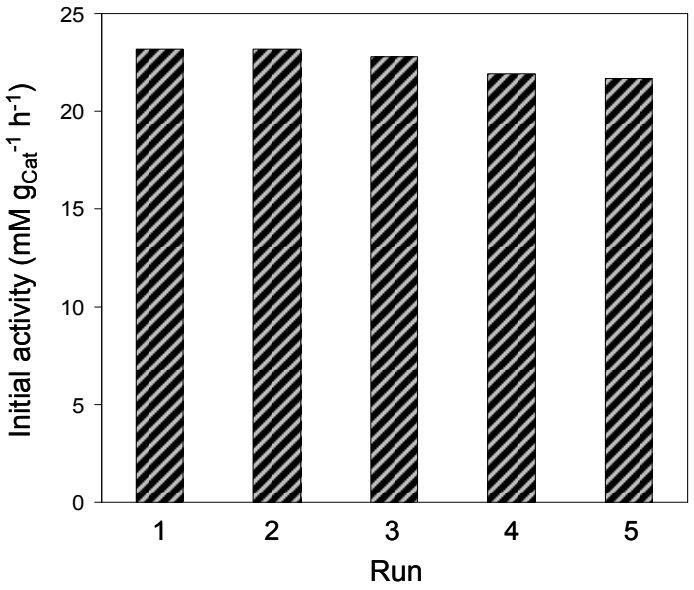

Palladium supported on amino functionalized magnetic MCM-41 for catalytic hydrogenation of aqueous bromate

Huan Chen [a], Peng Zhang [a], Wenhui Tan [a], Fang Jiang [a]*, Rong Tang [b]

[a] *Key Laboratory of Jiangsu Province for Chemical Pollution Control and Resources Reuse, School of Environmental & Biological Engineering, Nanjing University of Science and Technology, Nanjing 210094, PR China*

[b] *Jiangsu Open University, Nanjing 210036, PR China*

*Corresponding author. Tel: +86-25-84311819; Fax: +86-25-84315352.

E-mail: fjiang@njust.edu.cn (F. Jiang)

Abstract

Pd supported on amino functionalized magnetic MCM-41 was synthesized by deposition-precipitation (DP) and impregnation (IMP) methods. The catalysts were characterized by N_2 adsorption, XRD, FTIR, CO chemisorption, TEM, XPS and VSM. Liquid phase catalytic hydrogenation of bromate was tested over these catalysts. The results showed that DP catalyst had a higher activity than IMP catalyst, due to its higher Pd dispersion. As for DP catalysts supported on magnetic MCM-41 with different NH_2 loading amount, positive relationship was observed between Pd dispersion and the initial catalytic activity. Moreover, the DP-2 catalyst (supported on magnetic MCM-41 with 0.99 mmol of NH_2/g) was completely recovered with an external magnetic field, and the catalytic activity remained unaltered even after 5 repeated cycles for the bromate reduction.

Keywords: Catalytic hydrogenation; Pd supported on amino functionalized magnetic MCM-41; Deposition-precipitation method; Bromate; Pd dispersion

1. Introduction

Bromate is the main inorganic disinfection byproduct formed during the ozonation of bromide-containing water.[1,2] Due to its high toxicity, the United States Environmental Protection Agency (USEPA) and the World Health Organization have formulated the acceptable bromate levels of 0.01 mg L^{-1} in drinking water.[3,4] Thus, many effective treatment methods have been developed to remove bromate from drinking water, such as adsorption,[5] photocatalysis,[6] zero-valent iron reduction,[7] and recently catalytic hydrogenation.[8]

The catalytic hydrogenation method has been identified as a promising method for the removal of many contaminants from water, such as nitrate,[9] perchlorate[10], chlorophenol[11] and nitrophenol.[12] Noble metals have been extensively applied as catalysts in the hydrogenation process, and among them Pd is suggested as a highly active metal. Generally, the activity of supported Pd catalysts is related to the nature of active Pd, which is influenced by the property of support, method of preparation and nature of Pd precursor, etc.[13,14] In this case, many researchers have focused their attention on developing catalysts with high activity by improving the surface property of catalyst support. Employing functional group, such as amine or amino, onto the surface of catalyst, is an effective approach to modify the surface and electronic properties.[15] The amine or amino groups on catalyst support are well known to stabilize Pd nanoparticles against aggregation and to increase Pd dispersion.[16,17] Yi *et al.*[18] reported that an amine-functionalized silica supported Pd catalyst provided excellent reactivity and reusability in the hydrogenation of nitrobenzene. They interpreted that the phenomenon was resulted from the high Pd dispersion and the suppression of the aggregation of Pd nanoclusters during the hydrogenation process. Similarly, Mandal *et al.*[19] investigated a Pd nanoparticles immobilized on amine-functionalized zeolite catalyst, and observed a high activity and stability in the hydrogenation reaction. Besides of the surface property of catalyst support, the preparation method of catalyst is considered to be another important impact factor on catalytic behavior. Compared to conventional

impregnation (IMP) method, deposition-precipitation (DP) method is suggested to be a more appropriate method to produce catalysts with higher Pd dispersion. Hence, it is feasible to improve hydrogenation efficiency by applying this method to develop high dispersed Pd catalyst. As reported by Gopinath *et al.*,[20] the high activity of 1 wt% Pd/ZrO_2 catalyst prepared by the DP method in hydrodechlorination of chlorobenzene could be attributed to the high Pd dispersion.

Apart from the catalytic activity, another key challenge in the industrial application of hydrogenation is the reusability of catalysts. Therefore, developing catalysts which can be easily separated and recycled is highly desirable. One approach to such a problem is using magnetic materials as catalyst support. The catalyst supported on magnetic materials can be easily separated from the reaction solution by the application of an external magnetic field. For example, Guin *et al.*[21] prepared Pd supported amine-terminated Fe_3O_4 and $NiFe_2O_4$ catalysts for a series of hydrogenation reactions, and found that the catalysts could be completely recoverable by magnetic separation and the efficiency of the catalyst remained unaltered after 10 repeated cycles.

In the present investigation, magnetic Pd catalysts supported on amino functionalized MCM-41 with different NH_2 loading amount are developed by DP and IMP methods. A comparison is made between the activities of these catalysts on liquid phase catalytic hydrogenation of bromate. The variation in catalytic activity is interpreted based on the Pd dispersion.

2. Experimental

2.1 Catalyst Preparation

2.1.1 Preparation of magMCM-41 and magMCM-41-NH_2

The magnetic MCM-41 sample (magMCM-41) was prepared by a two-step synthesis procedure described by Chen *et al.*[22] In the first step, magnetic Fe_3O_4 nanoparticles were prepared as follows. 1.5 g of $FeCl_3$ and 0.6 g of $FeCl_2$ were dissolved in 10 mL of deionized water and deoxidized by N_2. Then, the mixture was added to 50 mL of 1.0 mol L^{-1} $NH_3 \cdot H_2O$ solution containing 0.2 g of

cetyltrimethylammonium bromide (CTAB) under sonication and N_2 protection. After reaction for 30 min, the Fe_3O_4 nanoparticles were recovered magnetically. In the second step, the magMCM-41 was prepared by adding the as-synthesized Fe_3O_4 nanoparticles to solution containing 640 mL of deionized water, 360 mL of 15 mol L^{-1} $NH_3 \cdot H_2O$ solution and 5.8 g of CTAB. Then, the suspension was refluxed for 30 min under vigorous stirring and N_2 atmosphere. Afterwards, 23.3 mL of tetraethylorthosilicate was added dropwise to the mixture and remained at 30 °C for 24 h. Finally, the obtained nanocomposite was magnetically collected and the organic template CTAB was removed by calcination at 550 °C for 5h under the protection of N_2. The resulting solid was referred to magMCM-41.

The amino functionalized magMCM-41 (magMCM-41-NH_2) was prepared by a post-grafting method. Typically, 2.0 g of magMCM-41 particles were suspended in 100 mL of dry toluene containing a certain amount of 3-aminopropyltrimethoxysilane (APTES). Then, the mixture was stirred under N_2 flow, and refluxed at 110 °C for 12 h. Finally, the magMCM-41-NH_2 sample was separated from the toluene solution by magnetic decantation, washed with ethanol and acetone for several times, and dried at 70 °C under vacuum for 12 h. Five different functionalized magMCM-41 samples were obtained by using different ratios of volume of APTES (ml) to mass of magMCM-41 (g). Samples with the ratio of 0.1, 0.25, 0.5, 1.0, and 2.0 were designated as magMCM-41N1, magMCM-41N2, magMCM-41N3, magMCM-41N4 and magMCM-41N5, respectively. The concentrations of amino group was calculated from nitrogen content obtained by elemental analyzer (CHN-O-Rapid, Heracus) were 0.83, 0.99, 1.19, 1.41 and 1.59 mmol/g for magMCM-41N1, magMCM-41N2, magMCM-41N3, magMCM-41N4 and magMCM-41N5, respectively. The unfunctionalized magMCM-41 was designated as magMCM-41N0.

2.1.2 Preparation of supported Pd catalysts

Supported Pd catalysts were prepared using deposition-precipitation (DP) and impregnation (IMP) method. In the DP method, palladium hydroxide was precipitated by the addition of 0.1 M Na_2CO_3 on magMCM-41 or magMCM-41-NH_2

support from $PdCl_2$ solution. The pH of the solution was maintained at 10.5 for 1 h. Afterwards, the solid was separated magnetically, washed several times with deionized water till no chloride ion was detected. In the IMP method, 0.5 g of the magMCM-41 or magMCM-41-NH_2 was impregnated with 1.67 g of 56.3 mM $PdCl_2$ solution (molar ratio NaCl:$PdCl_2$=2.5, pH 3-4). Then, the mixture was evaporated to dryness under stirring at 90 ^oC.

All of the samples made by DP and IMP were dried overnight and calcined at 200 ^oC for 2 h under a N_2 flow of 40 mL min^{-1}, and reduced at 200 ^oC for 4 h under a H_2 flow of 40 mL min^{-1}. All catalysts were ground to pass through a 400-mesh sieve (<37 μm) to ensure negligible intraparticular diffusion before bromate reduction.[23,24] The Pd contents of the obtained DP and IMP catalysts were around 2.0 % determined by X-ray fluorescence (ARL-9800). The DP catalysts using magMCM-41N1, magMCM-41N2, magMCM-41N3, magMCM-41N4 and magMCM-41N5 as support were designated as DP-1, DP-2, DP-3, DP-4, DP-5, respectively. The IMP catalysts using magMCM-41N1, magMCM-41N2, magMCM-41N3, magMCM-41N4 and magMCM-41N5 as support were designated as IMP-1, IMP-2, IMP-3, IMP-4, IMP-5, respectively. The catalysts prepared by unfunctionalized MCM-41 were designated as IMP-0 and DP-0, respectively.

2.2 Catalyst Characterization

BET surface areas of the catalysts were determined by N_2 adsorption method on Micromeritics ASAP 2200. The samples were pretreated at 200 ^oC under vacuum (1.33 Pa) for 4 h. X-ray diffraction (XRD) patterns of the catalysts were obtained by a powder diffraction-meter (D/max-RA, Rigaku), operating with a Cu anode at 30 kV and 20 mA. The Fourier transform infrared spectra (FTIR) spectra were acquired in transmission mode on a Nicolet Nexus 870 FTIR spectrophotometer in the range of 4000-400 cm^{-1}. The morphology and size of catalyst was obtained by a JEOL 2100 transmission electron microscope. X-ray photoelectron spectroscopy (XPS) was performed on a PHI 5000 VersaProbe XPS instrument using a monochromatized Al Kα excitation source (hν = 1486.6 eV). The magnetic properties of the catalysts were measured by a vibration sample magnetometry (VSM 7410).

Pd dispersion was evaluated using the CO chemisorption method. Typically, 100 mg of the reduced catalyst was activated under a H_2 flow of 40 mL min^{-1} at 200 ^oC for 2 h. After flushing by Ar flow (30 mL min^{-1}) for 1 h at 200 ^oC, the catalyst was cooled down to room temperature. The CO chemisorption was performed with pulses of 0.5 ml. In order to calculate the metal dispersion, an adsorption stoichiometry of Pd/CO =1 was assumed.[25]

2.3 Catalytic bromate reduction

Hydrogenation reduction of bromate was conducted at atmospheric pressure under 25 ^oC in a 250 ml three-necked flask reactor. Typically, a mixture of the catalyst (10.0 mg) and deionized water (180 ml) was placed in the reactor at first, and H_2 was introduced (40 mL min^{-1}) under stirring rate of 1000 rpm for 30 min. Then, 20 ml of 7.8 mM bromate solution was added rapidly, and the solution pH was 5.6 without adjustment. The samples were taken at the desired reaction time and the catalyst particles were filtered with a 0.45 μm membrane. Bromate and bromide concentration in the filtrate was determined by Ion Chromatography (ICS 2000, Dionex). The initial activities of the catalysts were calculated by the removal rate of the bromate within initial 7 min.

As shown in Fig. 1S (see Supporting information), the sum concentrations of bromate and bromide were nearly identical to the initial bromate concentrations during the reaction procedure, reflecting that bromide was the sole bromate reduction product by DP-2. The effect of mass transfer limitation under the reaction condition was evaluated. Bromate reduction over DP-2 with varied catalyst dosages and stirring rates was compared and the results were presented in Fig. 2S. As catalyst dosage and stirring rate increased, the initial activities were nearly constant, indicating that the reaction was absence of mass transfer limitation.[26,27]

3. Results and discussion

3.1 Catalyst characterization

3.1.1 BET surface area

The BET surface areas of DP and IMP catalysts are summarized in Table 1. The

amino functionalized DP catalysts appeared lower surface area than the unfunctionalized DP-0 catalyst, and increasing amount of silylating agent (APTES) during the functionalization of magMCM-41 resulted in a decrease of the surface area. The phenomenon was presumably due to the pores of functionalized catalysts were partially occupied by amino groups. The same results were found for IMP-0 and amino functionalized IMP catalysts.

3.1.2 XRD

Crystalline structures of the catalysts were analyzed by XRD. The wide-angle XRD for the magMCM-41, IMP-0, IMP-2, DP-0 and DP-2 samples are shown in Fig. 1a. The characteristic diffraction peaks at 2θ=30.1°, 35.3°, 43.0°, 56.9° and 62.5° assigned to magnetite were observable for all of the samples (JCPDS No. 19-692).[28] It demonstrated that all of the DP and IMP catalysts had been successfully synthesized without damaging the crystal structure of Fe_3O_4. Notably, diffraction peaks characteristic of Pd were not found in these catalysts, presumably because of the small Pd particle size.[29] Similar phenomenon was observed in the wide-angle XRD for the DP-1, DP-3, DP-4, DP-5, IMP-1, IMP-3, IMP-4 and IMP-5 in Fig. 3S.

As seen from the small-angle XRD patterns in Fig. 1b, the DP-0 catalyst exhibited three diffraction peaks corresponding to (100), (110), and (200) reflections, which assigned to the hexagonal mesoporous structure. After the amino modification, the intensities of the three peaks were reduced and the positions were slightly shifted towards higher value, revealing the decrease of the structural order in amino functionalized DP catalysts. The results were consistent with the XRD patterns of MCM-41 and MCM-41-NH_2 materials in previous literatures.[30,31]

3.1.3 FTIR

The FTIR spectra of DP catalysts were recorded to confirm the existence of magnetite and amino groups on the catalyst surface (Fig. 2). For DP-0 and amino functionalized DP catalysts, the intense peaks at 1103 cm^{-1} and 476 cm^{-1} were due to the Si-O stretching vibration and bending vibration in the amorphous silica shell, respectively. Additionally, the presence of magnetite nanoparticles was verified by the adsorption band at 590 cm^{-1}, corresponding to the Fe-O vibrations.[32] In the case

of amino functionalized DP catalysts, a series of weak peaks appeared at 1450-1600 cm^{-1} could be attributed to the deformation vibration of amino groups,[33] indicating that aminopropyl groups had been grafted to the catalyst surface.

3.1.4 Pd dispersion

The Pd dispersions of DP and IMP catalysts calculated from CO chemisorption are listed in Table 1. The Pd dispersions in DP catalysts were much higher than those in IMP catalysts, indicative of better Pd dispersion on DP catalysts. The difference in Pd species existed on the catalyst surface may be the main reason causing varied Pd dispersion in DP and IMP catalysts. For IMP catalysts, it was hard to eliminate the chloride species from the catalyst surface even after calcinations and reduction. Thus, they possessed low CO adsorption capacity. In the case of DP catalysts, the formation of $Pd(OH)_2$ in the catalyst surface might have facilitated metal-support interaction upon calcinations. This strong interaction inhibited the agglomeration of Pd particles on the catalyst surface, resulting in high Pd dispersion. Similar results were achieved in catalysts with other supports, such as CeO_2[20] and TiO_2.[34] Pd/CeO_2 or Pd/TiO_2 catalyst made by DP method showed higher dispersion than that by IMP method.

For DP catalysts before and after amino functionalization, it was clearly observed from Table 1 that DP-2 catalyst had much higher Pd dispersion than DP-0. This is because that during the procedure of catalyst preparation, the amino groups have large affinity with Pd precursor, hence suppress the agglomeration of Pd particles.[18] Furthermore, in comparison of DP catalysts with different surface concentration of amino groups, the volcano-type dependence of Pd dispersion on the NH_2 loading was observed. In detail, when the concentration of amino groups in magMCM-41 increased from 0 to 0.99 mmol/g, the Pd dispersion raised significantly from 39.40% to 84.23%. However, further increase in the concentration of amino groups decreased Pd dispersion.

3.1.5 TEM

The TEM images of the IMP-0, IMP-2, DP-0 and amino functionalized DP catalysts are shown in Fig. 3. Ordered mesostructures with hexagonal symmetry and

uniform pore dimension were clearly visible for all of the catalysts, confirming the hexagonal mesoporous structure speculated from XRD results. Additionally, uniform Pd particles were clearly identified for these catalysts. The average Pd particle sizes could be quantified using equation:[35]

$$\overline{d_s} = \sum n_i d_i^3 / \sum n_i d_i^2 \quad (1)$$

where n_i is the number of counted Pd particles with diameter of d_i, the total number of counted Pd particles($\sum n_i$) is larger than 100.

The average sizes of the Pd particles were calculated to be 2.80, 1.73, 1.40, 1.57, 2.33, 2.48, 5.33 and 4.98 nm for DP-0, DP-1, DP-2, DP-3, DP-4, DP-5, IMP-0 and IMP-2, respectively. The small Pd particle sizes on DP catalyst could be attributed to the effective Pd particle dispersion in the catalyst surface. Among the amino functionalized DP catalysts, the DP-2 owned the smallest Pd particle. It confirmed the result of CO chemisorption that DP-2 had the highest Pd dispersion.

3.1.6 XPS

The XPS results on the DP-0, DP-2, IMP-0 and IMP-2 catalysts are shown in Fig. 4. The N 1s binding energy value at 399.8 eV in DP-2 and IMP-2 corresponded to -NH_2. It confirmed that amino group had been grafted onto the surface of catalyst. The N 1s binding energy value at 399.8 eV was also observed in DP-1, DP-3, DP-4 and DP-5 in Fig 4S.

The Pd $3d_{5/2}$ binding energy value at 335.1 eV in DP-0 could be attributed to the presence of metallic Pd species, while the binding energy shifted to 336.1 eV in DP-2. It indicated that there was an interaction between Pd and amino group to make Pd more stable on the surface of DP-2 catalyst, thus suppress the agglomeration of Pd particles.[36] In the case of DP catalysts with different amount of amine groups, the binding energies were 336.1 eV, 336.1 eV, 336.0 eV, 335.9 eV and 335.7 eV for DP-1, DP-2, DP-3, DP-4 and DP-5, respectively (Fig 4S). The lower Pd $3d_{5/2}$ binding energy in DP-5 related to the attenuate interaction between Pd and amino groups, associated with the phenomenon of Pd agglomeration. The result was consistent with the result of Pd particle size that DP-5 owned the largest Pd particle

size among the texted catalysts. As for IMP-0 and IMP-2 catalysts, the Pd $3d_{5/2}$ binding energy was 335.4 eV, which corresponded to metallic Pd species. No significant interaction between Pd and the catalyst support was observed in IMP catalysts.

3.1.7 VSM

The magnetic hysteresis curves of DP-2 before and after reaction are shown in Fig. 5. The saturation magnetization of DP-2 before reaction was 6.22 emu g^{-1} and the coercivity was almost negligible, suggesting that the catalyst was superparamagnetic. The inset picture in Fig. 5 shows the magnetic separation of DP-2. It could be clearly seen that the catalyst was completely separated in an external magnetic field. As for DP-2 after reaction, the saturation magnetization value was 6.21 emu g^{-1}, and the catalyst could also be magnetic separated. It reflected that DP-2 after reaction remained superparamagnetic and the bromate reduction had little influence on magnetic property of the catalyst.

3.2. Catalytic bromate reduction

Catalytic bromate reduction as a function of reaction time over IMP-0, IMP-2, DP-0 and DP-2 is compiled in Fig. 6. The bromate reduction efficiencies were 31.4%, 31.9%, 40.0% and 100% for IMP-0, IMP-2, DP-0 and DP-2, respectively, indicating DP catalysts presented higher catalytic activities than IMP catalysts. The difference in catalytic activities caused by catalyst preparation method was related to Pd dispersion. A higher Pd dispersion resulted in more Pd active sites and active H, thus caused higher activity.

To further verify the effect of Pd dispersion, the catalytic hydrogenation of bromate over amino functionalized DP catalysts is compared in Fig. 7a. The bromate reduction efficiency increased from 40.0% to 100% when the concentration of amino groups increased from 0 (DP-0) to 0.99 mmol/g (DP-2), followed by a decline in activity with a further increase of NH_2 loading. More information obtained by revealing the relationship of initial catalytic activity and Pd dispersion was shown in Fig. 7b. As can be seen, increasing Pd dispersion created enhanced catalytic activity.

The reusability of catalyst is very important for the practical applications of

hydrogenation system. Therefore, the reusability of DP-2 catalyst is tested by repeated five runs at the same reaction condition. The DP-2 catalyst could be efficiently recycled for bromate reduction by magnetic separation. As shown in Fig. 8, the DP-2 catalyst could be reused five times without significant loss of activity performance (<6%) in the reduction of bromate. This indicated that the properties of Pd particles on the DP-2 catalyst had little change after the recycle reactions. Minor loss of catalytic activity was also observed in DP-1, DP-3, DP-4 and DP-5 catalysts after five repeated cycles (Fig 5S). Thus, the DP catalyst could be a promising reusable catalyst for catalytic hydrogenation of bromate.

4. Conclusions

Magnetic Pd catalysts supported on amino functionalized MCM-41 were prepared by deposition-precipitation (DP) and impregnation (IMP) methods. Characterization results revealed that DP catalysts possessed higher Pd dispersion than IMP catalysts. Liquid phase catalytic hydrogenation of bromate was tested over the as-made catalysts. The DP catalyst exhibited a higher activity than IMP catalyst, due to the higher Pd dispersion of DP catalyst. In addition, the initial catalytic activity for DP catalysts with varied NH_2 loading amount was also dependent on the Pd dispersion. In particular, the DP-2 catalyst could be easily recovered by magnet and the reusability was excellent for the bromate reduction. The results showed that the as-synthesized DP-2 catalyst was of great potential as an active and reusable catalyst for the catalytic reduction of bromate.

Acknowledgements

The financial supports from the Natural Science Foundation of China (No. 51208257 and 51178223), the Natural Science Foundation of Jiangsu Province (SBK201240759), China Postdoctoral Science Foundation (No. 2013M541677) and the Natural Science Fund for Colleges and Universities in Jiangsu Province (12KJB610002) are gratefully acknowledged.

References

1 U.V. Gunten, *Water Res*. 2003, **37**, 1469-1487.

2 Y. Nie, C. Hu, N. Li, L. Yang, J. Qu, *Appl. Catal. B: Environ.* 2014, **147**, 287-292.

3 H.S. Weinberg, C.A. Delcomyn, V. Unnam, *Environ. Sci. Technol*., 2003, **37**, 3104-3110.

4 World Health Organization. Bromate in drinking-water. Background document for preparation of WHO guidelines for drinking-water quality. World Health Organization Press, Geneva, 2005.

5 R. Chitrakar, Y. Makita, A. Sonoda, T. Hirotsu, *Appl. Clay. Sci.*, 2011, **51**, 375-379.

6 H. Noguchi, A. Nakajima, T. Watanabe, K. Hashimoto, *Environ. Sci. Technol.*, 2003, **37**, 153-157.

7 L.I. Xie, C. Shang, *Environ. Sci. Technol*., 2005, **39**, 1092-1100.

8 H. Chen, Z.Y. Xu, H.Q. Wan, J.Z. Zheng, D.Q. Yin, S.R. Zheng, *Appl. Catal. B: Environ.*, 2010, **96**, 307-313.

9 U. Prusse, K.D. Vorlop, *Mol. Catal. A: Chem.*, 2001, **173**, 313-328.

10 J.Y. Liu, J.K. Choe, Z. Sasnow, C.J. Werth, T.J., *Water Res.*, 2013, **47**, 91-101.

11 Z.J. Wu, C.X. Sun, Y. Chai, M.H. Zhang, *RSC Adv.*, 2011, **1**, 1179-1182.

12 Z.M. Wang, C.L. Xu, G.Q. Gao, X. Li, *RSC Adv.*, 2014, **4**, 13644-13651.

13 R. Gopinath, N.S. Babu, J.V. Kumar, N. Lingaiah, P.S.S. Prasad, *Catal. Lett.*, 2008, **120**, 312-319.

14 Y. Li, X. Xu, P.F. Zhang, Y.T. Gong, H.R. Li, Y. Wang, *RSC Adv*., 2013, **3**, 10973-10982.

15 F. Zhang, J. Jin, X. Zhong, S. Li, J. Niu, R. Li, J. Ma, *Green Chem.*, 2011, **13**, 1238-1243.

16 R. Abu-Reziq, D. Wang, M. Post, H. Alper, *Chem. Mater.*, 2008, **20**, 2544-2550.

17 A.J. Amali, R.K. Rana, *Green Chem.*, 2009, **11**, 1781-1786.

18 D.K. Yi, S.S. Lee, J.Y. Ying, *Chem. Mater.*, 2006, **18**, 2459-2461.

19 S. Mandal, D. Roy, R.V. Chaudhari, M. Sastry, *Chem. Mater.*, 2004, **16**, 3714-3724.

20 R. Gopinath, N. Lingaiah, B. Sreedhar, I. Suryanarayana, P.S. Sai Prasad, A. Obuchi, *Appl. Catal. B: Environ.*, 2003, **46**, 587-594.

21 D. Guin, B. Baruwati, S.V. Manorama, *Org. Lett.*, 2007, **9**, 1419-1421.

22 X. Chen, K.F. Lam, Q. Zhang, B. Pan, M. Arruebo, K.L. Yeung, *Phys. Chem. C.*, 2009, **113**, 9804-9813.

23 M.A. Aramendía, V. Boráu, I.M. García, C. Jiménez, F. Lafont, A. Marinas, J.M. Marinas, F.J. Urbano, *Mol. Catal. A: Chem.*, 2002, **184**, 237-245.

24 G. Yuan, M.A. Keane, *Chem. Eng. Sci.*, 2003, **58**, 257-267.

25 G. Neri, M.G. Musolino, C. Milone, D. Pietropaolo, S. Galvagno, *Appl. Catal. A: Gen.*, 2001, **208**, 307-316.

26 O.M. Ilinitch, F.P. Cuperus, L.V. Nosova, E.N. Gribov, *Catal. Today*, 2000, **56**, 137-145.

27 P. Zhang, F. Jiang, H. Chen, *Chem. Eng. J.*, 2013, **234**, 195-202.

28 J.H. Jang, H.B. Lim, *Microchem. J.*, 2010, **94**, 148.

29 Y.K. Hwang, D.Y. Hong, J.S. Chang, S.H. Jhung, Y.K. Seo, J. Kim, A. Vimont, C. Serre, G. Férey, *Angew. Chem. Int. Ed.*, 2008, **47**, 4144-4148.

30 D.B. Nale, S. Rana, K. Parida, B.M. Bhanage, *Appl. Catal. A: Gen.*, 2014, **469**, 340-349.

31 T. Joseph, K. Vijay Kumar, A.V. Ramaswamy, S.B. Halligudi, *Catal. Commun.*, 2007, **8**, 629-634.

32 M. Yamaura, R.L. Camilo, L.C. Sampaio, M.A. Macêdo, M. Nakamura, H.E. Toma, *J. Magn. Magn. Mater.*, 2004, **279**, 210-217.

33 K.M. Parida, D. Rath, *J. Mol. Catal. A: Chem.*, 2009, **310**, 93-100.

34 N.S. Babu, N. Lingaiah, N. Pasha, J.V. Kumar, P.S. Prasad, *Catal. Today*, 2009, **141**, 120-124.

35 G. Yuan, M.A. Keane, *Appl. Catal. B: Environ.*, 2004, **52** 301-314.

36 M. Ma, Q. Zhang, D. Yin, J. Dou, H. Zhang, H. Xu, *Catal. Commun.*, 2012, **17** 168-172.

Figure captions

Fig. 1. (a) Wide-angle XRD patterns of DP-0, DP-2, IMP-0, IMP-2, magMCM-41 and (b) low-angle XRD patterns of DP-0 and amino functionalized DP catalysts.

Fig. 2. FTIR spectra of DP-0 and amino functionalized DP catalysts.

Fig. 3. TEM images of (a) DP-0, (b) DP-1, (c) DP-2 (d) DP-3, (e) DP-4, (f) DP-5, (g) IMP-0 and (h) IMP-2.

Fig. 4. XPS spectra of N 1s and Pd 3d for DP-0, DP-2, IMP-0 and IMP-2 catalysts.

Fig. 5. Magnetization curves and magnetic separation pictures (insert) of DP-2 before and after bromate reduction reaction.

Fig. 6. Catalytic bromate reduction over DP-0, DP-2, IMP-0 and IMP-2 catalysts.

Fig. 7. (a) Catalytic bromate reduction over amino functionalized DP catalysts and (b) initial catalytic activity of amino functionalized DP catalysts as a function of Pd dispersion.

Fig. 8. Reusability of DP-2 catalyst for bromate reduction.